AJR FOCUS ON: AJR WOMEN'S IMAGING

MRI, CT, and PET/CT for Ovarian Cancer Detection and Adnexal Lesion Characterization

Veena R. Iyer[1]
Susanna I. Lee

OBJECTIVE. The purpose of this article is to describe the role of MR, CT, and PET/CT in the detection of ovarian cancer and the evaluation of adnexal lesions.

CONCLUSION. The goal of imaging in ovarian cancer detection is to expeditiously distinguish benign adnexal lesions from those requiring further pathologic evaluation for malignancy. For lesions indeterminate on ultrasound, MRI increases the specificity of imaging evaluation, thus decreasing benign resections. CT is useful in diagnosis and treatment planning of advanced cancer. Although ^{18}F-FDG-avid ovarian lesions in postmenopausal women are considered suspicious for malignancy, PET/CT is not recommended for primary cancer detection because of high false-positive rates.

Ovarian cancer is the leading cause of death from gynecologic cancers, with 21,550 estimated new cases and 14,600 estimated deaths in the United States in 2009 [1]. The lifetime risk of dying from invasive ovarian cancer is about one in 95. If diagnosed at stage I (ovary confined), there is a greater than 90% survival rate at 5 years. At the time of diagnosis, the majority of patients (65–70% of cases) are found to have stage III (upper abdominal or regional lymph node metastases) or stage IV (extraabdominal or hematogenous metastases) disease with a 5-year survival rate of 30–73% [2]. Because early stage at diagnosis is correlated with a better prognosis, screening trials using transvaginal ultrasound have been undertaken with the hope of facilitating early detection.

Incidentally discovered adnexal masses are common. In the United States, there is a 5–10% lifetime risk of women undergoing surgery for this indication [3]. Incidental lesions pose a challenging diagnostic problem because imaging features of benign and malignant adnexal masses overlap [4]. Although most incidental adnexal masses are benign [3], surgery rather than long-term follow-up may be indicated if imaging features cannot definitively characterize the lesion as benign, depending on the patient's age and other risk factors for malignancy [5]. However, oophorectomy, although a relatively minor surgical procedure, is also associated with long-term adverse consequences. Surgical peritubal adhesions are associated with hydrosalpinx and infection. Unilateral oophorectomy can shorten a woman's reproductive span by decreasing ovarian reserve [6]. Bilateral oophorectomy results in morbidity and mortality of premature menopause, including accelerated bone loss and cardiovascular death [7, 8]. Thus, once an adnexal lesion has been detected, the goal of further imaging is accurate tissue characterization resulting in surgery only for lesions that are indeterminate or frankly malignant.

This article describes the role of MRI, CT, and PET/CT in the detection of ovarian cancer and the evaluation of adnexal lesions. The biology of ovarian cancer and the natural history of adnexal masses relevant to imaging detection are reviewed. The relative usefulness and diagnostic accuracy of each technique in the imaging workup is discussed. Ovarian cancers of both common and rare histologies as well as other adnexal pathologies are presented with correlative imaging on multiple techniques.

Biology of Ovarian Tumors: Implications for Imaging Detection

Tumors arising from the surface epithelium account for 90% of ovarian cancers and are pathologically designated as serous, mucinous, clear cell, endometrioid, or Brenner (transitional) tumors based on the cell type. Each histologic type is further classified as

Keywords: borderline tumor, endometriosis, gynecology, Krukenberg tumor, screening, staging

DOI:10.2214/AJR.09.3522

Received August 24, 2009; accepted after revision October 23, 2009.

[1]Both authors: Department of Radiology, Massachusetts General Hospital, Harvard Medical School, 55 Fruit St., White 270, Boston, MA 02114. Address correspondence to V. R. Iyer (viyer@partners.org).

AJR 2010; 194:311–321

0361–803X/10/1942–311

benign, borderline malignant (tumors of low malignant potential), or malignant, reflecting differences in clinical behavior [9]. Borderline tumors are more frequently diagnosed in young women [10], and management decisions require that the relatively low risk of tumor-related mortality be balanced against considerations of operative risks, fertility preservation, and long-term morbidity of premature menopause if a complete cancer operation is pursued.

The most common malignant epithelial tumor cell type is serous cystadenocarcinoma, which is histologically divided into low grade and high grade [11]. Rather than representing a spectrum, these two groups likely represent distinct diagnoses, displaying different epidemiology, pathogenesis, and clinical course [12]. High-grade serous carcinoma, the most commonly encountered cancer in clinical practice, arises de novo from the ovarian surface epithelium from an unknown precursor lesion and progresses rapidly. In contrast, the less-common low-grade serous tumors develop in a stepwise fashion from known precursor lesions and display a less rapidly aggressive pattern of spread, even at stages III and IV [13]. Nevertheless, both types are lethal, with the 5-year survival for low-grade and high-grade carcinomas reported as 55% [14] and 30% [12], respectively.

Because the most common ovarian cancer is high-grade serous cystadenocarcinoma, screening trials using transvaginal ultrasound have established that the majority of ovarian cancers show rapid progression from early-stage sonographically detectable lesion to stage III disease (Fig. 1). In one study, high-grade ovarian cancers all grew within 4–6 weeks, with an estimated doubling time of less than 3 months [15]. In another trial that imaged women every 6 months with transvaginal ultrasound, all 10 of the ovarian cancers detected were at stage III or IV, having developed within the 6-month interval between screenings [16]. Given the observed rapid doubling time of ovarian cancer and its propensity for extraovarian dissemination, consensus recommendations state that if imaging cannot quickly characterize an adnexal lesion as benign, or if clinical indicators or patient risk factors suggest cancer, the lesion should be resected rather than followed [17].

Ovarian cancer screening trials have also revealed that, in the general population, adnexal lesions are common, whereas ovarian cancer is relatively rare [18, 19] (Table 1). In one study that followed more than 15,000 asymptomatic postmenopausal women over an average period of 6.3 years, 18% developed unilocular cysts (measuring up to 10 cm) of which 69% resolved spontaneously [20]. Complex ovarian cysts show a reported incidence of 3.2% in postmenopausal women, 55% of which resolve within 60 days [15]. This high incidence of benign adnexal lesions coupled with the low incidence of ovarian cancer in the general population means that a diagnostic test with 100% sensitivity and 99% specificity is estimated to have a positive predictive value of 4.8% [17]. In other words, more than 95% of lesions resected on the basis of such a test would be benign.

Incidental adnexal masses represent a wide variety of pathologies [21] (Table 2), including functional cysts, infectious processes, endometriosis, benign or malignant neo-

TABLE 1: Incidence of Incidental Adnexal Masses

Menstrual Status [Reference]	Ultrasound Features	Prevalence (%)	Estimated Risk of Malignancy (%)
Postmenopausal [18]	Simple cyst (< 10 cm)	3.3	0 to < 0.1
Premenopausal [19]	Simple cyst	15.0	NA
Postmenopausal [18]	Complex cyst (< 10 cm)	3.2	6.1

Note—NA indicates not applicable.

TABLE 2: Differential Diagnosis of Adnexal Lesions [21]

Location	Lesion Type	Differential Diagnosis
Ovarian		
	Benign lesions	
		Endometrioma
		Physiologic cyst: simple or hemorrhagic
		Cystadenoma: serous, mucinous
		Mature cystic teratoma or dermoid
		Stromal tumor: fibroma, thecoma
	Borderline and malignant lesions	
	Epithelial	
		Serous carcinoma
		Mucinous carcinoma
		Clear cell carcinoma
		Endometrioid carcinoma
		Brenner or transitional cell carcinoma
	Nonepithelial	
		Germ cell tumors (e.g., dysgerminoma, yolk sac, embryonal)
		Sex-cord stromal tumors (e.g., granulosa cell tumor, Sertoli-Leydig tumor)
		Rare histologies (e.g., carcinosarcoma, primitive neuroectodermal tumor, lymphoma)
		Metastasis (e.g., breast, colon, gastric, pancreatic)
Extraovarian		
	Predominantly solid	
		Fibroid: pedunculated uterine or broad ligament
	Predominantly cystic	Endometrioma
		Fallopian tube: hydrosalpinx, hematosalpinx, pyosalpinx
		Peritoneal inclusion cyst
		Paratubal cyst

plasms, and masses originating from adjacent pelvic organs such as the uterus or bowel. Transvaginal ultrasound is the preferred technique for initial evaluation because of its availability, high resolution, and lack of ionizing radiation. A wide range of sensitivities and specificities, 85–100% and 52–100%, respectively, has been reported for detection of ovarian malignancies using ultrasound [22–28]. Factors such as operator expertise and patient body habitus are thought to account for this variability. There is currently no validated, sufficiently accurate, and cost-effective screening test for early detection of ovarian cancer. Because the goal of the imaging workup is expeditious and accurate triage, a second test that would better characterize adnexal lesions that are indeterminate on ultrasound has been sought.

MRI

A meta-analysis evaluating the incremental value of a second test for an indeterminate adnexal mass detected on gray-scale ultrasound determined that MRI with IV contrast administration provided the highest posttest probability of ovarian cancer when compared with CT, Doppler ultrasound, or MRI without contrast administration [29] (Table 3). When used for further evaluation of an indeterminate mass seen on ultrasound in a prospective series, contrast-enhanced MRI showed sensitivity and specificity of 100% and 94%, respectively, in diagnosis of malignancy [30]. Although MRI can be helpful in cancer detection, the preponderant contribution of MRI in adnexal mass evaluation is its specificity because it provides confident diagnosis of many common benign adnexal lesions [29]. In a prospective study of women with suspected adnexal masses, both Doppler ultrasound and MRI were highly sensitive for identifying malignant lesions (ultrasound 100%, MRI 96.6%), but the specificity of MRI was significantly greater (ultrasound 39.5%, MRI 83.7%). Therefore, women who clinically have a low risk of malignancy but have indeterminate lesions on ultrasound are the ones most likely to benefit from MRI [31].

MRI is useful for definitively diagnosing many common benign adnexal lesions. MRI better characterizes indeterminate adnexal lesions seen on ultrasound, especially if an extraovarian cystic lesion is suspected but a normal ipsilateral ovary is not seen and if a predominantly solid lesion requires more tissue-specific characterization for diagnosis. Cystic extraovarian lesions include peritoneal inclusion cysts, paratubal cysts, and hydrosalpinx. Solid-appearing adnexal lesions include dermoids, exophytic uterine and broad ligament fibroids, and ovarian fibrothecomas. Finally, MRI is a valuable tool in characterizing a complex cystic ovarian mass as an endometrioma and may detect signs of relatively rare malignant degeneration within it.

Epithelial Ovarian Tumors

The MRI features of high-grade malignancies (Fig. 2) are analogous to those seen with ultrasound and CT [32]. Typically, they are predominantly cystic lesions with solid components, such as septae, mural nodules, and papillary projections. The primary criteria for diagnosis of malignancy are large solid component, wall thickness greater than 3 mm, septal thickness greater than 3 mm and/or nodularity, and necrosis. Ancillary criteria that serve to definitively characterize a tumor as malignant include involvement of pelvic organs or sidewall; peritoneal, mesenteric, or omental disease; ascites; and adenopathy. When these criteria are used, the sensitivities and specificities for malignancy range between 91–92% and 91–100%, respectively [32, 33].

Borderline tumors (Fig. 3) are rarely diagnosed preoperatively because they lack diagnostic imaging features that distinguish them from benign or early malignant epithelial tumors. On MRI, borderline tumors are predominantly cystic, with fluid ranging in T1 and T2 signal because of varying concentrations of protein and mucin. There may be numerous solid mural nodules or thick septa that enhance with gadolinium contrast administration [34]. There is no evidence of lymphadenopathy, ascites, or peritoneal implants [35]. The diagnosis can be suggested on the basis of these features in a younger patient with normal or only mildly elevated CA-125 levels [36].

Cystic Extraovarian Lesions

When a cystic adnexal mass can be shown to be separate from the ipsilateral ovary (extraovarian), it is usually benign. Early fallopian tube carcinoma presenting when tube-confined represents a very rare exception. The most common causes are peritoneal inclusion cysts, paratubal or paraovarian cysts, and hydrosalpinges. An intact ipsilateral ovary may not be identified with transvaginal ultrasound because of overlying bowel or because it is out of the field of view. In such cases, MRI is often helpful in visualizing the normal ovary and confirming the extraovarian nature of the lesion (Fig. 4).

Peritoneal inclusion cysts arise from pelvic adhesions that result from prior infections, surgery, or endometriosis. Fluid that is normally produced by the ovaries is trapped by the surrounding adhesions resulting in T1-hypointense and T2-hyperintense collections with thick or thin septations. Peritoneal inclusion cysts characteristically assume the shape of the space within which they lie rather than displacing surrounding structures. The intact ovary and broad ligament are often surrounded by septated fluid collections [37].

Paratubal cysts are common developmental variants arising from mesonephric or paramesonephric duct remnants in the broad ligament. They are usually single, but occasionally they are multiple unilocular cysts arising from the fimbriated end of the tube [38] and can be very large, measuring up to 28 cm in diameter. On MRI, they are typically homogeneously T1-hypointense and T2-hyperintense lesions with no solid components but may sometimes appear complex from prior hemorrhage or infection [39].

Hydrosalpinx arises from blockage of a fallopian tube and is usually secondary to infection, surgery, or endometriosis. The tube can often enlarge to greater than 10 cm in size. On MRI, hydrosalpinx appears as a C- or S-shaped cyst and is characterized by in-

TABLE 3: Accuracy of Ovarian Cancer Diagnosis in Adnexal Masses Indeterminate on Ultrasound [29]

Transvaginal Ultrasound Followed by	Sensitivity (%)	Specificity (%)
Doppler ultrasound	84 (81–87)	82 (79–85)
CT	81 (73–85)	87 (81–94)
Unenhanced MRI	76 (70–82)	97 (95–98)
Contrast-enhanced MRI	81 (77–84)	98 (97–99)

Note—Data in parentheses indicate 95% CI.

complete longitudinal folds representing the partially effaced mucosal plicae of the fallopian tube. These can sometimes be mistaken for mural nodules when the tube is markedly dilated [40]. Uncomplicated hydrosalpinx shows homogeneous T1 hypointensity and T2 hyperintensity of simple fluid. However, the signal intensity of the fluid can vary greatly when the dilated tube is filled with pus (pyosalpinx) or blood (hematosalpinx).

Predominantly Solid Adnexal Lesions

Benign tumors such as fibroids, fibrothecomas, and dermoids comprise the majority of the predominantly solid adnexal lesions encountered incidentally. Ovarian cancer, usually cystadenocarcinoma that is typically mixed cystic and solid, is rarely confused with these lesions. However, the less-common histologic types of primary ovarian malignancies, such as Brenner tumor, dysgerminoma, or granulosa cell tumor (Fig. 5), can appear predominantly solid [41]. On MRI, they can sometimes be distinguished from the benign lesions because they originate from the ovary (unlike a fibroid), show heterogeneity in tissue signal and enhancement (unlike fibrothecoma), and show no fatty tissue (unlike a dermoid).

Fibroids (leiomyomas) are benign neoplasms composed of smooth-muscle cells and fibrous connective tissue arranged in a whorl-like pattern. Although most originate in the uterine myometrium, smooth muscle tumors histologically indistinguishable from fibroids have been observed separate from the uterus arising in the broad ligament, other pelvic and upper abdominal organs, the peritoneal and retroperitoneal cavities, and the thorax [42]. Pedunculated uterine subserosal and broad-ligament fibroids frequently present as adnexal masses. MRI helps in the diagnosis of these lesions by showing their extraovarian location and their connection to the uterus or the broad ligament. Fibroids can undergo various types of degeneration, such as cystic, hyaline, mucinous, myxomatous, fatty, and carneous (red), resulting in a wide range of observed MRI signal intensities. Fibroids can be low to high signal on T1- or T2-weighted images and hypervascular to nonvascular on dynamic contrast-enhanced imaging [43, 44]. The common MRI features of fibroids are that they are round, well-demarcated, displace rather than infiltrate surrounding structures, and often show homogeneous signal intensity and pattern of enhancement.

Fibromas, thecomas, and fibrothecomas are solid benign ovarian tumors arising from sex cord and stromal cells. Fibromas are made up of bundles of benign fibroblasts and collagen arranged in whorls. Thecomas are composed of theca cells with abundant cytoplasmic lipid and varying fibrosis. The term "fibrothecoma" reflects the frequently observed histologic overlap [45]. On MRI, their characteristic feature is internal homogeneity on all pulse sequences, with low signal on both T1- and T2-weighted images and mild enhancement with gadolinium administration. Fibrothecomas can be differentiated from fibroids whenever the latter can be seen as separate from the ovary [46]. Fibrothecomas can sometimes be hormonally active, producing estrogen and causing endometrial hyperplasia or malignancy (Fig. 6). A triad of fibroma with ascites and plural effusion, which clinically mimics ovarian cancer but resolves after resection of the tumor, is called Meigs syndrome [47].

Mature cystic teratomas, commonly referred to as dermoids, are composed of well-differentiated ectodermal, endodermal, and mesodermal germ layers. The gross pathologic appearance of dermoids is usually that of a unilocular cyst with a solid Rokitansky nodule that is composed of fat and hair. Histologically, the cyst is lined with squamous epithelium and filled with sebaceous material. On MRI, the presence of macroscopic fat, which shows T1-hyperintense signal with signal loss on fat-suppression sequences, is diagnostic for a dermoid. Chemical shift artifact is seen in 62–87% of cases [48–50].

Endometrioma and Malignant Transformation of Endometriosis

The presence of endometrial glands and stroma outside the uterus is defined as endometriosis. The ovary is the most commonly involved site, where cysts termed "chocolate cysts" or "endometriomas" are seen. Cyclic bleeding results in the accumulation of blood products of different ages within the cysts that contain very high concentrations of paramagnetic products of hemoglobin breakdown. As a result, endometriomas are typically lightbulb-bright lesions on fat-suppressed T1-weighted images. Although a wide range of T2 signal intensity has been observed, ranging from a fluid hyperintensity to complete signal void, low-signal-intensity shading [51] has been reported as characteristic. The presence of concurrent T1-hyperintense extraovarian implants of endometriosis is also helpful in making the diagnosis of an ovarian endometrioma. Endometriomas can appear complex, containing solid debris, clot, or calcification. The typically thin cyst wall shows contrast enhancement but, when fibrotic, can appear thick and irregular, mimicking malignancy.

Malignant transformation is estimated to occur in 0.6–0.8% of women with ovarian endometriosis [52–54]. The pathogenesis is unclear, but long-term exposure to unopposed estrogen is thought to play a role. Endometrioid and clear cell adenocarcinomas are the most common histologic types. On MRI, the most important finding for detecting malignant transformation of an endometrioma is the presence of enhancing mural nodules [55, 56]. Unenhanced and contrast-enhanced subtraction imaging are valuable in detecting small enhancing nodules within the background of a T1-hyperintense endometrioma [56] (Fig. 7). In pregnancy, however, mural nodules appear within endometrial cysts due to benign decidual changes in endometrial tissue that can simulate secondary neoplasm [56–58]. Mural nodules suggesting malignant degeneration can be differentiated from debris or blood clots adherent to the cyst wall by the lack of contrast enhancement in the latter. Adjacent enhancing ovarian parenchyma can be differentiated from mural nodules by their extracystic location and crescentic shape, and are best seen on T2-weighted images.

CT

In the United States, CT is often the first technique with which ovarian cancer is detected. Because presenting symptoms of ovarian cancer indicate advanced disease and are typically nonspecific (e.g., abdominal pain or distention, urinary frequency, early satiety), CT is obtained to evaluate for occult intraabdominal malignancy or ascites. Advanced ovarian cancer on CT typically presents as cysts with thick walls, septations, and papillary projections that are more clearly seen after contrast administration. Ancillary findings of pelvic organ or sidewall invasion, peritoneal implants, adenopathy, and ascites increase the confidence for diagnosing malignancy [4]. Although this pattern of disease is typical for ovarian cancer, other cancers—such as colon, gastric, and pancreatic cancer—with ovarian metastases also can present similarly (Figs. 8 and 9). Because ovarian cancer is treated with surgical cytoreduction even with peritoneal or lymphatic involvement, the radiologist should try to distinguish ovarian cancer from other tumors that may have similar presentations but require nonsurgical treatment.

CT is the preferred technique in the pretreatment evaluation of ovarian cancer to define the extent of disease and assess the likelihood of optimal surgical cytoreduction. Tumor involvement of the diaphragm and the large bowel mesentery has been shown to be the most reliable CT predictor of suboptimal cytoreduction, although other features such as suprarenal paraaortic adenopathy; omental tumor extending into the spleen, stomach, or lesser sac; tumor growth into the pelvic sidewall; and hydroureter, are also associated with a poor surgical result [5]. CT has been shown to predict suboptimal cytoreduction with sensitivity of 79% and specificity of 75%. However, accuracy varies considerably among institutions, likely reflecting variations in surgical practice and technique as well as differing definitions of optimal cytoreduction [59]. For predicting correct stage, the sensitivity and specificity of CT were reported to be 50% and 92%, respectively, in one series [60].

PET/CT

The use of ^{18}F-FDG PET imaging, with reported sensitivity of 52–58% and specificity of 76–78%, is not recommended for primary detection of ovarian cancer [61, 62]. False-negative results have been reported with borderline tumors and low-grade and early adenocarcinomas. False-positive results have been reported with hydrosalpinges, pedunculated fibroids, and endometriosis [61, 63]. In premenopausal women undergoing surveillance imaging for other malignancies, hypermetabolic ovarian uptake is seen in the late follicular to early luteal cyst [64] (Fig. 10) and has been mistaken for metastases to the ovaries or the pelvic sidewall nodes [65–68]. In contrast, hypermetabolic ovarian uptake in a postmenopausal woman is abnormal and should be considered suspicious for malignancy (Fig. 11). Thus, in interpreting PET images, ovarian tracer uptake should be correlated with the patient's menstrual status and phase [69].

Although not a preferred technique for cancer detection, PET/CT is playing an expanding role in treatment planning and follow-up. For predicting the correct stage, the addition of PET to contrast-enhanced CT has been shown to improve accuracy [70–72]. FDG PET, again combined with CT, is the most accurate technique to evaluate for suspected recurrent ovarian cancer [73–75]. A meta-analysis comparing techniques for detection of recurrence determined that PET/CT (sensitivity, 91%; specificity, 88%) performed better than CT (sensitivity, 79%; specificity, 84%) or MRI (sensitivity, 75%; specificity, 78%) [76]. Hypermetabolic tumor implants, especially in subdiaphragmatic or subhepatic locations, on the serosal surfaces of the bowel, or in small nodes, are more conspicuous with PET than with conventional imaging. Conversely, lack of high-level tracer uptake in posttreatment findings (e.g., fat necrosis, seroma, reactive nodal enlargement) decreases the false-positive rate. In addition, with fusion PET/CT, the CT images provide high-resolution, measurable information on the extent of disease and the anatomic sites of involvement for treatment planning and follow-up.

Conclusion

Incidental adnexal masses are common in both pre- and postmenopausal women with the vast majority being benign. Ultrasound is the study of choice for primary evaluation of adnexal masses, and MRI and CT are useful for further workup and to define extent of disease. Lesions that are indeterminate on ultrasound can often be characterized with greater specificity by contrast-enhanced MRI as definitively benign. Symptomatic ovarian cancer that has spread out of the ovary often presents on CT, and it should be distinguished by the radiologist from a metastatic colon, or gastric or pancreatic cancer. CT is also the preferred technique in the pretreatment evaluation of ovarian cancer, to define the extent of disease, and to assess the likelihood of optimal surgical cytoreduction. Although FDG PET/CT is not recommended for primary ovarian cancer detection, hypermetabolic ovarian uptake in a postmenopausal woman is abnormal and should be considered suspicious for malignancy. In ovarian cancer patients with suspected recurrence, PET/CT is the best technique for lesion detection and treatment follow-up.

References

1. American Cancer Society Website. Cancer facts and figures 2009. www.cancer.org/downloads/STT/500809web.pdf. Accessed July 17, 2009
2. Horner MJ, Ries LAG, Krapcho M, et al. SEER cancer statistics review. National Cancer Institute Website. seer.cancer.gov/csr/1975_2006/. Based on November 2008 SEER data submission, posted to the SEER Website, 2009. Accessed July 20, 2009
3. McDonald JM, Modesitt SC. The incidental postmenopausal adnexal mass. *Clin Obstet Gynecol* 2006; 49:506–516
4. Jeong YY, Outwater EK, Kang HK. Imaging evaluation of ovarian masses. *RadioGraphics* 2000; 20:1445–1470
5. Bristow RE, Duska LR, Lambrou NC, et al. A model for predicting surgical outcome in patients with advanced ovarian carcinoma using computed tomography. *Cancer* 2000; 89:1532–1540
6. Lass A. The fertility potential of women with a single ovary. *Hum Reprod Update* 1999; 5:546–550
7. Gotlieb WH, Chetrit A, Menczer J, et al. Demographic and genetic characteristics of patients with borderline ovarian tumors as compared to early stage invasive ovarian cancer. *Gynecol Oncol* 2005; 97:780–783
8. Shuster LT, Gostout BS, Grossardt BR, Rocca WA. Prophylactic oophorectomy in premenopausal women and long-term health. *Menopause Int* 2008; 14:111–116
9. Scully RE. *International histological classification of tumors: histological typing of ovarian tumors.* Geneva, Switzerland: World Health Organization, 1999
10. Barakat RR. Borderline tumors of the ovary. *Obstet Gynecol Clin North Am* 1994; 21:93–105
11. Malpica A, Deavers MT, Lu K, et al. Grading ovarian serous carcinoma using a two-tier system. *Am J Surg Pathol* 2004; 28:496–504
12. Shih IM, Kurman RJ. Ovarian tumorigenesis: a proposed model based on morphological and molecular genetic analysis. *Am J Pathol* 2004; 164:1511–1518
13. Gershenson DM, Sun CC, Lu KH, et al. Clinical behavior of stage II–IV low-grade serous carcinoma of the ovary. *Obstet Gynecol* 2006; 108:361–368
14. Smith Sehdev AE, Sehdev PS, Kurman RJ. Noninvasive and invasive micropapillary (low-grade) serous carcinoma of the ovary: a clinicopathologic analysis of 135 cases. *Am J Surg Pathol* 2003; 27:725–736
15. van Nagell JR Jr, DePriest PD, Reedy MB, et al. The efficacy of transvaginal sonographic screening in asymptomatic women at risk for ovarian cancer. *Gynecol Oncol* 2000; 77:350–356
16. Fishman DA, Cohen L, Blank SV, et al. The role of ultrasound evaluation in the detection of early-stage epithelial ovarian cancer. *Am J Obstet Gynecol* 2005; 192:1214–1221
17. American College of Obstetricians and Gynecologists. ACOG committee opinion: number 280, December 2002. The role of the generalist obstetrician-gynecologist in the early detection of ovarian cancer. *Obstet Gynecol* 2002; 100:1413–1416
18. Bailey CL, Ueland FR, Land GL, et al. The malignant potential of small cystic ovarian tumors in women over 50 years of age. *Gynecol Oncol* 1998; 69:3–7
19. Gerber B, Müller H, Külz T, Krause A, Reimer T. Simple ovarian cysts in premenopausal patients.

Int J Gynaecol Obstet 1997; 57:49–55

20. Modesitt SC, Pavlik EJ, Ueland FR, DePriest PD, Kryscio RJ, van Nagell JR Jr. Risk of malignancy in unilocular ovarian cystic tumors less than 10 centimeters in diameter. *Obstet Gynecol* 2003; 102:594–599
21. Zaloudek CF. Ovary, fallopian tube and broad and round ligaments. In: Fletcher CDM, ed. *Diagnostic histopathology of tumors*. Philadelphia, PA: Churchill Livingstone Elsevier, 2007:567–652
22. Buy JN, Ghossain MA, Hugol D, et al. Characterization of adnexal masses: combination of color Doppler and conventional sonography compared with spectral Doppler analysis alone and conventional sonography alone. *AJR* 1996; 166:385–393
23. Kurjak A, Predanic M. New scoring system for prediction of ovarian malignancy based on transvaginal color Doppler sonography. *J Ultrasound Med* 1992; 11:631–638
24. Brown DL, Doubilet PM, Miller FH, et al. Benign and malignant ovarian masses: selection of the most discriminating gray-scale and Doppler sonographic features. *Radiology* 1998; 208:103–110
25. Bromley B, Goodman H, Benacerraf BR. Comparison between sonographic morphology and Doppler waveform for the diagnosis of ovarian malignancy. *Obstet Gynecol* 1994; 83:434–437
26. Alcazar JL, Jurado M. Using a logistic model to predict malignancy of adnexal masses based on menopausal status, ultrasound morphology, and color Doppler findings. *Gynecol Oncol* 1998; 69:146–150
27. Caruso A, Caforio L, Testa AC, Ciampelli M, Panici PB, Mancuso S. Transvaginal color Doppler ultrasonography in the presurgical characterization of adnexal masses. *Gynecol Oncol* 1996; 63:184–191
28. Rehn M, Lohmann K, Rempen A. Transvaginal ultrasonography of pelvic masses: evaluation of B-mode technique and Doppler ultrasonography. *Am J Obstet Gynecol* 1996; 175:97–104
29. Kinkel K, Lu Y, Mehdizade A, Pelte MF, Hricak H. Indeterminate ovarian mass at US: incremental value of second imaging test for characterization—meta-analysis and Bayesian analysis. *Radiology* 2005; 236:85–94
30. Adusumilli S, Hussain HK, Caoili EM, et al. MRI of sonographically indeterminate adnexal masses. *AJR* 2006; 187:732–740
31. Sohaib SA, Mills TD, Sahdev A, et al. The role of magnetic resonance imaging and ultrasound in patients with adnexal masses. *Clin Radiol* 2005; 60:340–348
32. Stevens SK, Hricak H, Stern JL. Ovarian lesions: detection and characterization with gadolinium enhanced MR imaging at 1.5 T. *Radiology* 1991; 181:481–488
33. Hricak H, Chen M, Coakley FV, et al. Complex adnexal masses: detection and characterization with MR imaging—multivariate analysis. *Radiology* 2000; 214:39–46
34. Bazot M, Daraï E, Nassar-Slaba J, Lafont C, Thomassin-Naggara I. Value of magnetic resonance imaging for the diagnosis of ovarian tumors: a review. *J Comput Assist Tomogr* 2008; 32:712–723
35. Bent CL, Sahdev A, Rockall AG, Singh N, Sohaib SA, Reznek RH. MRI appearances of borderline ovarian tumours. *Clin Radiol* 2009; 64:430–438
36. Skírnisdóttir I, Garmo H, Wilander E, Holmberg L. Borderline ovarian tumors in Sweden 1960–2005: trends in incidence and age at diagnosis compared to ovarian cancer. *Int J Cancer* 2008; 123:1897–1901
37. Kim JS, Lee HJ, Woo SK, Lee TS. Peritoneal inclusion cysts and their relationship to the ovaries: evaluation with sonography. *Radiology* 1997; 204:481–484
38. Kim JS, Woo SK, Suh SJ, Morettin LB. Sonographic diagnosis of paraovarian cysts: value of detecting a separate ipsilateral ovary. *AJR* 1995; 164:1441–1444
39. Outwater EK, Scheibler ML. Magnetic resonance imaging of the ovary. *Magn Reson Imaging Clin N Am* 1994; 2:245–274
40. Kim MY, Rha SE, Oh SN, et al. MR imaging findings of hydrosalpinx: a comprehensive review. *RadioGraphics* 2009; 29:495–507
41. Imaoka I, Wada A, Kaji Y, et al. Developing an MR imaging strategy for diagnosis of ovarian masses. *RadioGraphics* 2006; 26:1431–1448
42. Cohen DT, Oliva E, Hahn PF, Fuller AF Jr, Lee SI. Uterine smooth-muscle tumors with unusual growth patterns: imaging with pathologic correlation. *AJR* 2007; 188:246–255
43. Hricak H, Tscholakoff D, Heinrichs L, et al. Uterine leiomyoma: correlation of MR, histopathologic findings, and symptoms. *Radiology* 1986; 158:385–391
44. Yamashita Y, Torashima M, Takahashi M, et al. Hyperintense uterine leiomyoma at T2-weighted MR imaging: differentiation with dynamic enhanced MR imaging and clinical implications. *Radiology* 1993; 189:721–725
45. Outwater EK, Wagner BJ, Mannion C, McLarney JK, Kim B. Sex cord stromal and steroid cell tumors of the ovary. *RadioGraphics* 1998; 18:1523–1546
46. Outwater EK, Siegelman ES, Talerman A, Dunton C. Ovarian fibromas and cystadenofibromas: MRI features of the fibrous component. *J Magn Reson Imaging* 1997; 7:465–471
47. Meigs JV, Cass JW. Fibroma of the ovary with ascites and hydrothorax: with a report of seven cases. *Am J Obstet Gynecol* 1937; 33:249–267
48. Togashi K, Nishimura K, Itoh K, et al. Ovarian cystic teratomas: MR imaging. *Radiology* 1987; 162:669–673
49. Imaoka I, Sugimura K, Okizuka H, Iwanari O, Kitao M, Ishida T. Ovarian cystic teratomas: value of chemical fat saturation magnetic resonance imaging. *Br J Radiol* 1993; 66:994–997
50. Stevens SK, Hricak H, Campos Z. Teratomas versus cystic hemorrhagic adnexal lesions: differentiation with proton-selective fat-saturation MR imaging. *Radiology* 1993; 186:481–488
51. Woodward PJ, Sohaey R, Mezzetti TP Jr. Endometriosis: radiologic–pathologic correlation. *RadioGraphics* 2001; 21:193–216
52. Heaps JM, Nieberg RK, Berek JS. Malignant neoplasms arising in endometriosis. *Obstet Gynecol* 1990; 75:1023–1028
53. Corner GW Jr, Hu C, Hertig AT. Ovarian carcinoma arising in endometriosis. *Am J Obstet Gynecol* 1950; 59:760–774
54. Scully RE, Richardson GS, Barlow JF. The development of malignancy in endometriosis. *Clin Obstet Gynecol* 1966; 9:384–411
55. Takeuchi M, Matsuzaki K, Uehara H, Nishitani H. Malignant transformation of pelvic endometriosis: MR imaging findings and pathologic correlation. *RadioGraphics* 2006; 26:407–417
56. Tanaka YO, Yoshizako T, Nishida M, Yamaguchi M, Sugimura K, Itai Y. Ovarian carcinoma in patients with endometriosis: MR imaging findings. *AJR* 2000; 175:1423–1430
57. Tamai K, Koyama T, Saga T, et al. MR features of physiologic and benign conditions of the ovary. *Eur Radiol* 2006; 16:2700–2711
58. Tanaka YO, Shigemitsu S, Nagata M, et al. A decidualized endometrial cyst in a pregnant woman: a case observed with a steady-state free precession imaging sequence. *Magn Reson Imaging* 2002; 20:301–304
59. Axtell AE, Lee MH, Bristow RE, et al. Multi-institutional reciprocal validation study of computed tomography predictors of suboptimal primary cytoreduction in patients with advanced ovarian cancer. *J Clin Oncol* 2007; 25:384–389
60. Forstner R, Hricak H, Occhipinti KA, Powell CB, Frankel SD, Stern JL. Ovarian cancer: staging with CT and MR imaging. *Radiology* 1995; 197:619–626
61. Fenchel S, Grab D, Nuessle K, et al. Asymptomatic adnexal masses: correlation of FDG PET and histopathologic findings. *Radiology* 2002; 223:780–788
62. Rieber A, Nussle K, Stohr I, et al. Preoperative diagnosis of ovarian tumors with MR imaging: comparison with transvaginal sonography, positron emission tomography, and histologic findings. *AJR* 2001; 177:123–129
63. Woodward PJ, Hosseinzadeh K, Saenger JS. From the archives of the AFIP: radiologic staging of ovarian carcinoma with pathologic correlation. *RadioGraphics* 2004; 24:225–246

64. Nishizawa S, Inubushi M, Okada H. Physiological ^{18}F-FDG uptake in the ovaries and uterus of healthy female volunteers. *Eur J Nucl Med Mol Imaging* 2005; 32:549–556
65. Ames J, Blodgett T, Meltzer C. ^{18}F-FDG uptake in an ovary containing a hemorrhagic corpus luteal cyst: false-positive PET/CT in a patient with cervical carcinoma. *AJR* 2005; 185:1057–1059
66. Bagga S. A corpus luteal cyst masquerading as a lymph node mass on PET/CT scan in a pregnant woman with an anterior mediastinal lymphomatous mass. *Clin Nucl Med* 2007; 32:649–651
67. Ho KC, Ng KK, Yen TC, Chou HH. An ovary in luteal phase mimicking common iliac lymph node metastasis from a primary cutaneous peripheral primitive neuroectodermal tumor as revealed by 18-fluoro-2-deoxyglucose positron emission tomography. *Br J Radiol* 2005; 78:343–345
68. Cottrill HM, Fitzcharles EK, Modesitt SC. Positron emission tomography in a premenopausal asymptomatic woman: a case report of increased ovarian uptake in a benign condition. *Int J Gynecol Cancer* 2005; 15:1127–1130
69. Kim SK, Kang KW, Roh JW, Sim JS, Lee ES, Park SY. Incidental ovarian ^{18}F-FDG accumulation on PET: correlation with the menstrual cycle. *Eur J Nucl Med Mol Imaging* 2005; 32:757–763
70. Schwarz JK, Grigsby PW, Dehdashti F, Delbeke D. The role of ^{18}F-FDG PET in assessing therapy response in cancer of the cervix and ovaries. *J Nucl Med* 2009; 50[suppl 1]:64S–73S
71. Kitajima K, Murakami K, Yamasaki E, et al. Diagnostic accuracy of integrated FDG-PET/contrast-enhanced CT in staging ovarian cancer: comparison with enhanced CT. *Eur J Nucl Med Mol Imaging* 2008; 35:1912–1920
72. Javitt MC. ACR Appropriateness Criteria on staging and follow-up of ovarian cancer. *J Am Coll Radiol* 2007; 4:586–589
73. Yoshida Y, Kurokawa T, Kawahara K, et al. Incremental benefits of FDG positron emission tomography over CT alone for the preoperative staging of ovarian cancer. *AJR* 2004; 182:227–233
74. Sebastian S, Lee SI, Horowitz NS, et al. PET–CT vs. CT alone in ovarian cancer recurrence. *Abdom Imaging* 2008; 33:112–118
75. Hauth EA, Antoch G, Stattaus J, et al. Evaluation of integrated whole-body PET/CT in the detection of recurrent ovarian cancer. *Eur J Radiol* 2005; 56:263–268
76. Gu P, Pan LL, Wu SQ, Sun L, Huang G. CA 125, PET alone, PET-CT, CT and MRI in diagnosing recurrent ovarian carcinoma: a systematic review and meta-analysis. *Eur J Radiol* 2009; 71:164–174

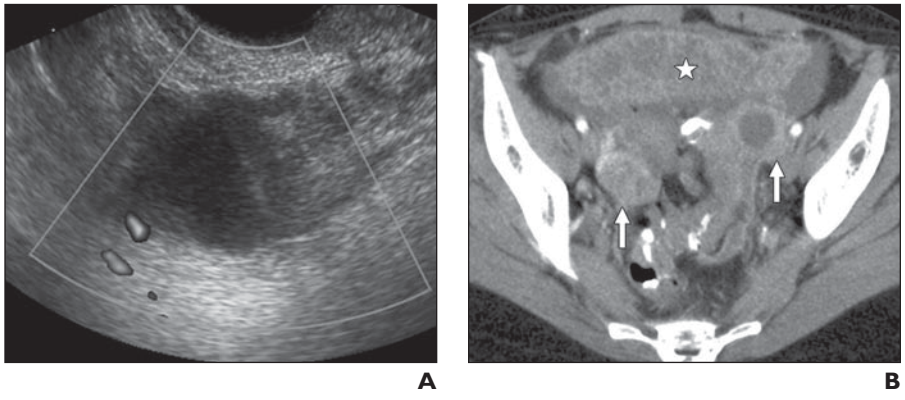

Fig. 1—Imaging in 42-year-old woman to show ovarian cancer rate of growth.
A, Transvaginal ultrasound image reveals incidental 2.4-cm complex left ovarian cyst. Right ovary was normal, and no ascites was seen (not shown).
B, Contrast-enhanced CT image obtained 7 weeks after **A** reveals bilateral mixed solid and cystic ovarian masses (*arrows*), omental cake (*star*), and ascites. Pathology revealed high-grade cystadenocarcinoma originating in left ovary.

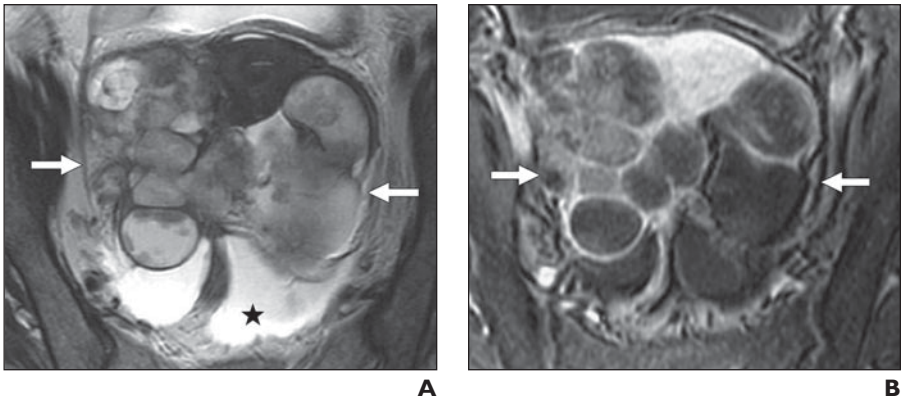

Fig. 2—Serous adenocarcinoma of ovary in 68-year-old woman.
A and **B,** Fast spin-echo T2-weighted (**A**) and gadolinium-enhanced (**B**) axial MR images reveal bilateral > 8-cm complex cystic adnexal masses (*arrows*) that show enhancing T2-isointense solid components. Large amount of ascites (*star*, **A**) is also noted.

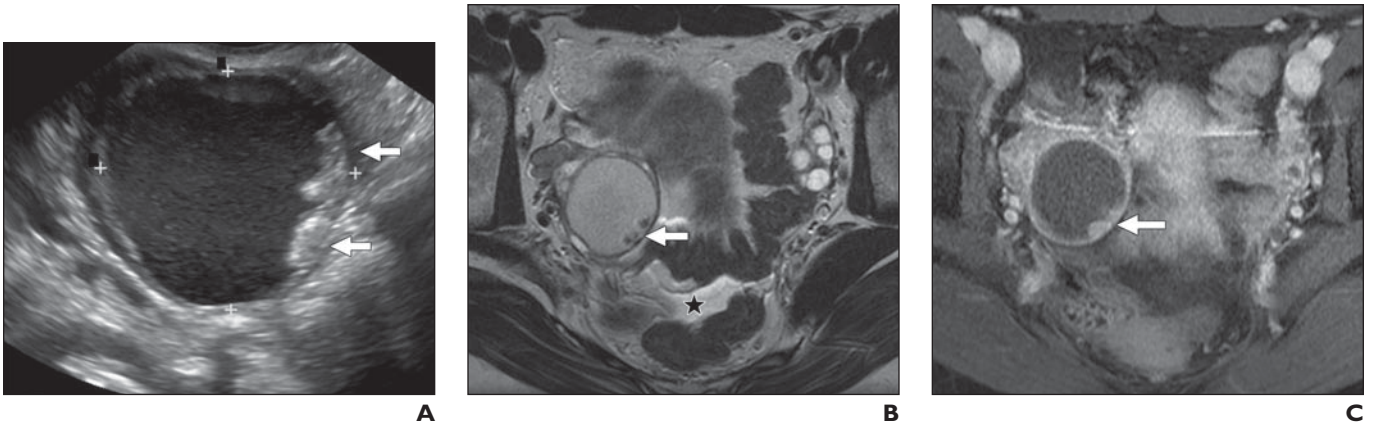

Fig. 3—Serous borderline tumor of ovary in 28-year-old woman.
A, Transvaginal ultrasound image reveals 3.5-cm cystic lesion with mural nodularity (*arrows*).
B and **C,** Fast spin-echo T2-weighted (**B**) and gadolinium-enhanced (**C**) axial MR images show solid nodules (*arrows*) enhancing with contrast material. Trace physiologic amount of free fluid (*star*, **B**) is noted.

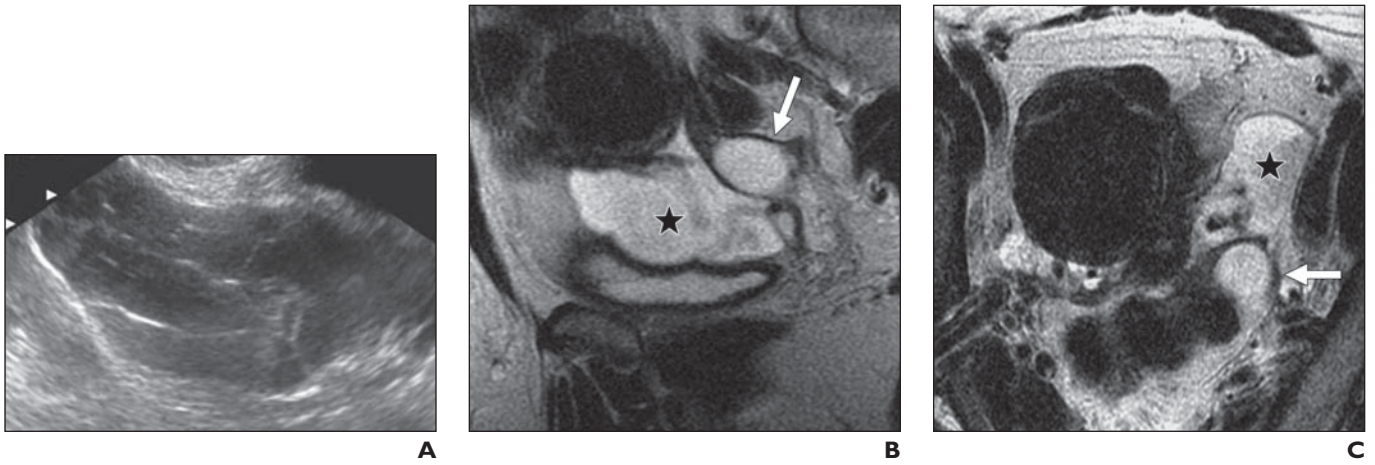

Fig. 4—Peritoneal inclusion cyst in 45-year-old woman with previous right oophorectomy.
A, Transvaginal ultrasound image reveals 5.5-cm cystic lesion with thick and thin septations. Normal left ovary was not seen.
B and **C,** Fast spin-echo T2-weighted sagittal (**B**) and axial (**C**) MR images reveal loculated collection of fluid (*star*) surrounding normal left ovary (*arrow*).

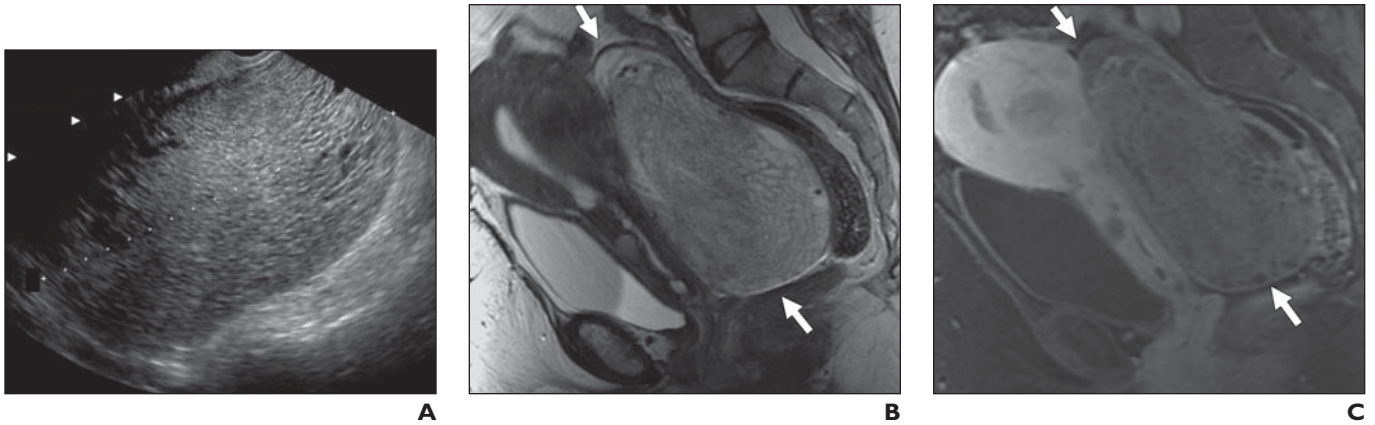

Fig. 5—Granulosa cell tumor in 44-year-old woman.
A, Transvaginal ultrasound image reveals 13-cm predominantly solid-appearing mass. Uterus and left ovary were unremarkable (not shown). Normal right ovary was not seen.
B and **C,** On fast spin-echo T2-weighted (**B**) and gadolinium-enhanced (**C**) sagittal MR images, mass (*arrows*) arises from right adnexa and is composed of both enhancing solid and microcystic components. No normal right ovarian tissue was seen.

Fig. 6—Hormone-producing fibrothecoma in 59-year-old woman with postmenopausal bleeding.
A, Transvaginal ultrasound image reveals 6-cm solid mass in right pelvis. Uterus and left ovary were normal (not shown). Normal right ovary was not seen.
B, Fast spin-echo T2-weighted coronal MR image shows that homogeneously hypointense solid mass originates from right ovary (*arrow*).
C, Gadolinium-enhanced sagittal MR image shows nearly homogeneous low-level enhancement of right ovarian mass (*arrow*). Heterogeneously enhancing lesion is also seen in endometrial cavity (*arrowhead*), which proved to be endometrial cancer resulting from long-term estrogen production of fibrothecoma.

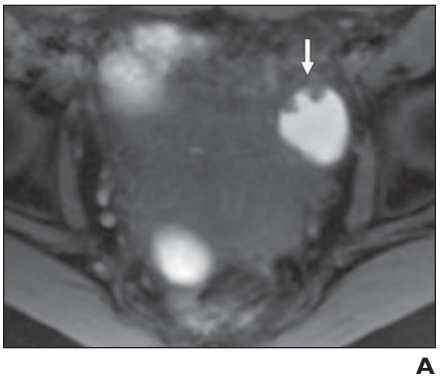

Fig. 7—Endometrioid adenocarcinoma arising in endometrioma in 36-year-old woman.
A, Axial T1-weighted MR image with fat saturation shows multiple lightbulb-bright lesions of endometriosis. Left ovarian endometrioma shows solid mural nodules (*arrow*).
B–D, Sagittal subtraction MR images (**B,** unenhanced; **C,** gadolinium-enhanced; and **D,** subtracted) show that mural nodules (*arrowheads*) enhance.

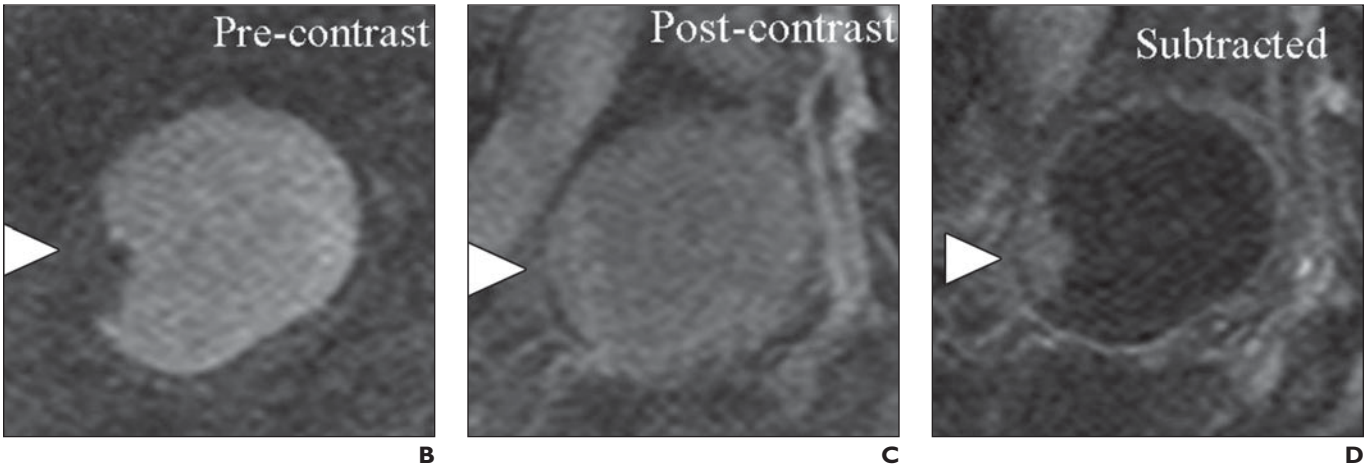

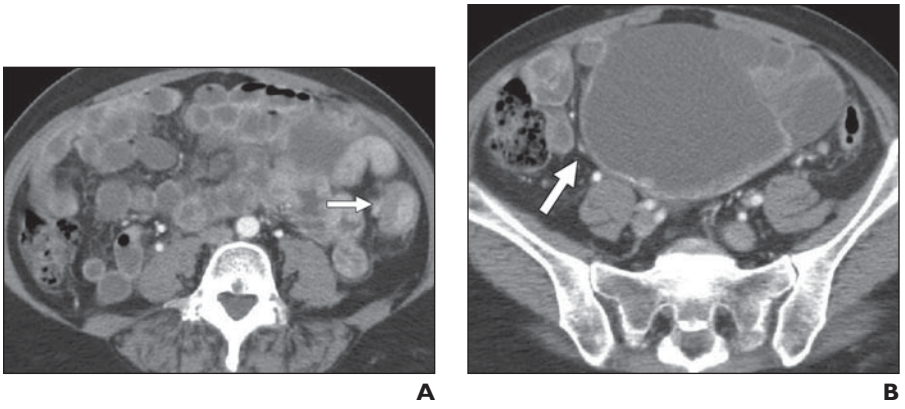

Fig. 8—Colon cancer metastatic to ovary in 58-year-old woman.
A and **B,** Contrast-enhanced CT image at level of mid abdomen (**A**) reveals eccentric focal thickening of mid descending colon (*arrow*), shown to be primary adenocarcinoma on colonoscopic biopsy. Pelvic CT image (**B**) from same examination reveals 15-cm right adnexal mass (*arrow*) that is predominantly cystic with enhancing nodular septa and that, on resection, proved to be metastatic colon cancer.

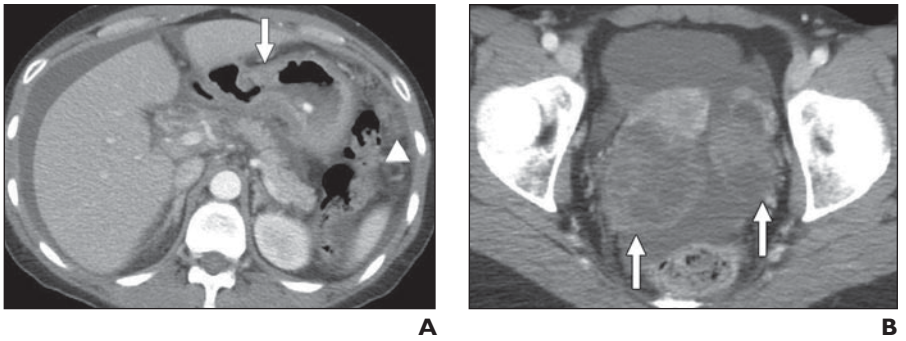

Fig. 9—Gastric cancer metastatic to ovaries in 42-year-old woman.
A, Contrast-enhanced CT image through upper abdomen reveals diffuse nodular gastric wall thickening (*arrow*) shown to be primary adenocarcinoma on endoscopic biopsy. Intraperitoneal tumor implants (*arrowhead*) and large amount of ascites also are noted.
B, Pelvic CT image from same examination as **A** reveals bilateral > 5-cm mixed solid and cystic adnexal masses (*arrows*), which were histologically confirmed to be metastatic gastric cancer.

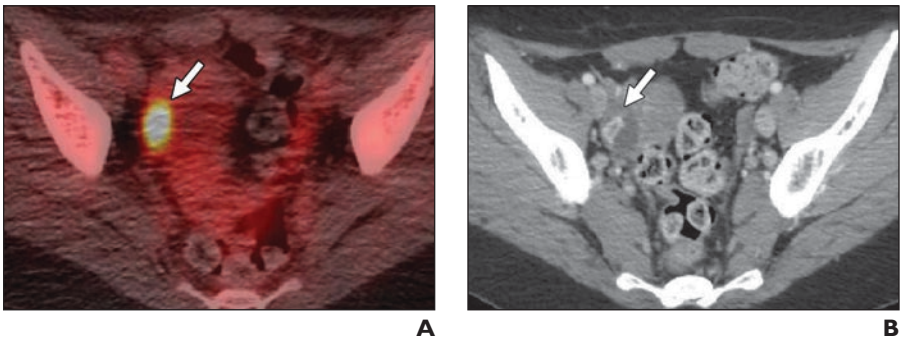

Fig. 10—Corpus luteum cyst in 33-year-old woman on day 14 of menstrual cycle.
A and **B,** PET/CT fusion image (**A**) through pelvis shows right adnexal hypermetabolic focus (*arrow*). Concurrent contrast-enhanced CT image (**B**) localizes ^{18}F-FDG activity to corpus luteum cyst (*arrow*).

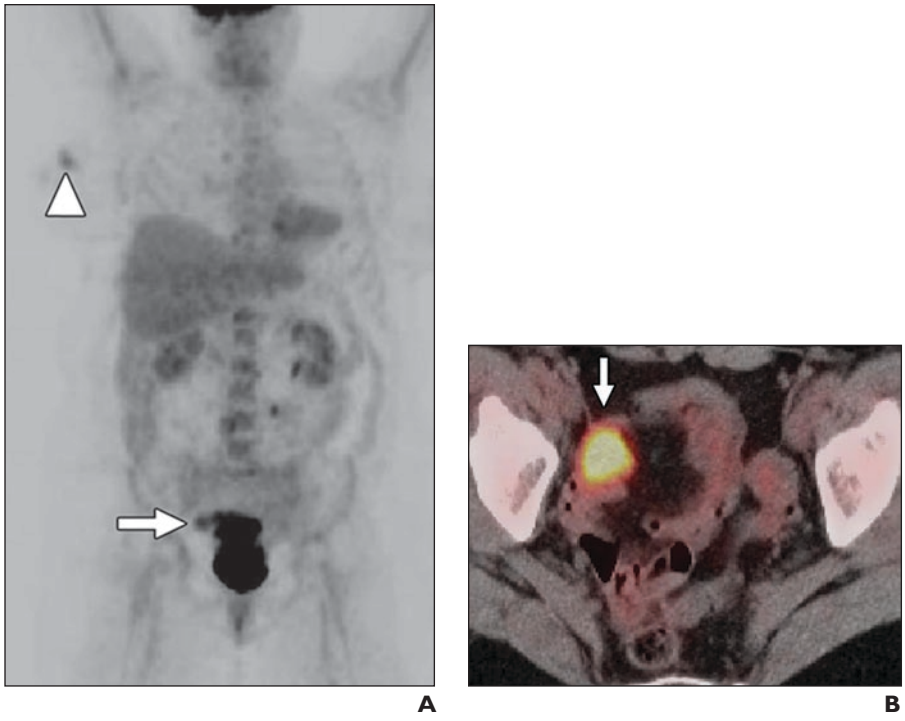

A B

Fig. 11—Incidental ovarian cancer in 59-year-old woman.
A, PET coronal whole-body image reveals two hypermetabolic foci, one in right breast (*arrowhead*) corresponding to known breast cancer and second in right pelvis (*arrow*).
B, PET/CT fusion image from same examination as **A** localizes pelvic hypermetabolic focus to right ovary (*arrow*), which on resection was shown to contain ovarian serous carcinoma.